Adult sex ratio as an index for male strategy

Danya Rose[a], Kristen Hawkes[b], Peter S. Kim[a]

[a]*School of Mathematics and Statistics, University of Sydney, Sydney, NSW 2006, Australia*

[b]*Department of Anthropology, University of Utah, Salt Lake City, UT 84112, USA*

Abstract

The adult sex ratio (ASR) is defined as the number of eligible males divided by the number of fertile females in a population. We build an ODE model with minimal age structure, in which males compete for paternities using either a multiple-mating or searching-then-guarding strategy, to investigate the value of ASR as an index for predicting which strategy males will adopt. Parameters in the model characterise aspects of life history and behaviour. Sensitivity analysis on the model parameters informs us that ASR is strongly influenced by parameters characterising life history, while dominant strategy is affected most strongly by the effectiveness of guarding (average length of time a guarded pair persists, and resistance to paternity theft) and moderately by some life history traits. For fixed effectiveness of guarding and other parameters, dominant strategy tends to change from multiple mating to guarding along a curve that aligns well with a contour of constant ASR, under variation of parameters such as longevity and age female fertility ends. This confirms the hypothesis that ASR may be a useful index for predicting the optimal male mating strategy, provided we have some limited information about ecology and behaviour.

1. Introduction

The closest living genus to our human genus, *Homo*, is genus *Pan*; and we share many physiological, developmental and behavioural traits with them. Significant differences exist, however, particularly regarding life history and the social structure around mating arrangements. While both humans and chimpanzees engage in a variety of strategies, such as multiple mating, possessive short term, or longer-lasting exclusive relationships (see, for example, [11]), each species tends to engage in one class of strategies with greater frequency than the others. Some recent studies examine the evolution of monogamy from a mathematical perspective; for example, [7, 8, 9, 10] all discuss the role of mating sex ratio and partner availability in the evolution of monogamy or other mating-related behaviour. In our study, we broadly categorise the reproductive strategies as either multiple mating or mate guarding, in order to build a relatively simple model that captures sufficient dynamics to explore the problem of predicting strategy by observing demography. Specifically, chimpanzees (with relatively more females per male) typically engage in multiple mating more frequently than guarding, and hunter-gatherers (with relatively scarce fertile females) tend to engage in guarding more frequently than multiple mating.

Life tables indicate that roughly half of infants in wild chimpanzee and hunter-gatherer groups will die before reaching adulthood (sexual maturity). Once reaching adulthood paths diverge: a chimpanzee just at maturity (first birth around age 14) may expect to live another fifteen to twenty years [4], but a human hunter-gatherer at the same point (first birth around age 19)

may expect to live healthily for another forty years or more [1, 5, 6]. The age of last birth occurs in both humans and chimps at around 45 years, almost no wild chimpanzee can expect to survive until this age; those who do, though robust enough to have reached that age, are by that time relatively frail. In stark contrast, many hunter-gatherer females live in good health beyond menopause, only becoming frail into their seventies; those who survive so long have spent half their adult lives post-fertile.

Though pair bonding is not unknown amongst the primates, humans are unique among great apes in that we tend to form relatively long-lasting pair bonds, as opposed to multiple mating, wherein no long term attachments are made. A favoured hypothesis to explain our different behaviour is that it arises from paternal investment, but more recent work suggests that other mechanisms may be responsible for this change of behaviour from our relatives. The extension of the human life span (and of the male eligibility period) without lengthening female fertility to later ages directly changes the ratio of eligible males to fertile females (called the adult sex ratio: ASR). As the ASR increases, the number of fertile females available per male decreases, which we argue changes the incentives for adopting either strategy.

In this paper, we construct a simple two-strategy ODE model, in which males either guard mates (once acquired) or multiply mate (that is, possibly acquiring many mates at the same time), and competition between strategies occurs only through the acquisition of paternities. Children are assumed to inherit the strategies of their fathers. Guarding males do not contribute to the survival of their offspring, and females do not express preference for either type of male. Our model has a number of parameters, which correspond to aspects of life history, ecology, and behaviour. We will vary the parameters and record the resulting dominant male strategy and the resulting ASR, with the intent to determine whether, or under what circumstances, the ASR can serve as an index for determining what strategy males are most likely to employ.

2. Population and life cycle

Consider a population P comprising

- eligible searching males G, who guard their mates once paired,
- eligible multiple-mating males M, who return to the mating pool as soon as they have mated,
- fertile receptive females F, who may be "recruited" by a G or M male and may or may not have been previously recruited,
- fertile unreceptive females F^M, who have been recruited by a multiple-mating male and are thus occupied short term by that male, or pregnant or lactating as a consequence,
- guarded pairs F^G, consisting of one eligible guarding male whose energy goes into (possibly imperfectly) guarding his mate from multiple maters and one fertile female who may bear offspring to multiple maters who steal paternities from her partner,
- children of guarding males C^G (called "guarded children"), and
- children of multiple-mating males C^M (called "unguarded children", though may be born to guarded females),

summarised in Table 1. The total population is $P = F + G + M + 2F^G + F^M + C^G + C^M$, where the number of guarded pairs F^G is counted twice because each guarded pair contains two individuals. Parameters of the model are summarised in Table 2, and its dynamics illustrated in Figure 1, and all are described below.

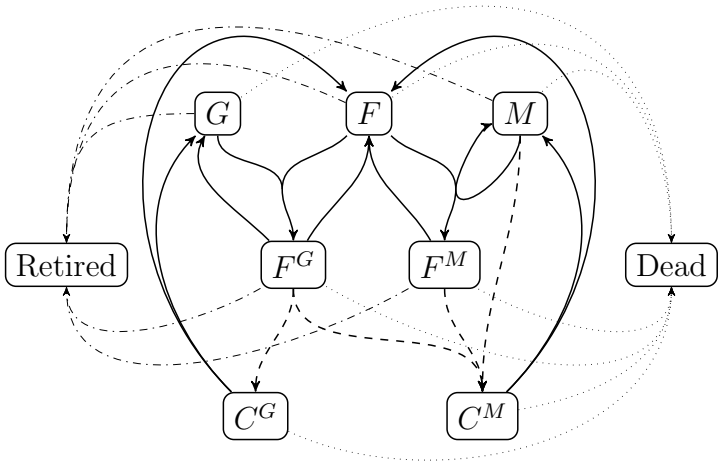

Figure 1: Illustration of our model. Solid lines denote movement of individuals between groups, dashed lines indicate contribution to a group, dash-dot lines indicate removal through retirement, and dotted lines indicate removal through death.

Children are assumed to mature to adulthood at rate γ per child, and die at rate δ per child (assumed independent of population density). Half the children who survive to maturity become receptive females, while the other half become either multiple maters or searchers (respectively the same as their fathers). Observe that paternal investment is not modelled here. Unguarded children do not receive less care than guarded children, and no distinction is made among the survival of children depending on their paternity. We do not attempt to address this question at all.

Fertile females include receptive and unreceptive females, and female members of guarded pairs. They die at base rate (assumed independent of population density) μ and advance to menopause at rate τ. Post-fertile females "retire" from the population as they reach menopause, as they no longer play a role in the reproductive dynamics in this model. We do not explicitly model grandmother effects. Eligible males include searching males, multiple-mating males and the male partners in guarded pairs. Eligible males have a base death rate of $k\mu$, and retire due to geriatric infirmity at rate λ, whereupon they too leave the population.

Receptive females are "recruited" by either searching or multiple-mating males at rate r per possible pair. If recruited by a searching male, they together form a guarded pair, which will on average break spontaneously with rate β per pair, with both partners returning to their respective original pools. Guarded pairs may also be broken by the death or retirement of one partner, in which case the remaining partner returns to his or her own original pool. Females recruited by multiple-mating males become unreceptive for a period of time, returning to the

Table 1: List and descriptions of all variables.

Variable	Description
P	Total population
F	Receptive females
G	Searching (guarding) males
M	Multiple-mating males
F^G	Guarded pairs
F^M	Unreceptive females
C^G	Guarded children
C^M	Unguarded children

receptive pool with average rate σ. Females in guarded pairs and unreceptive females produce children (respectively guarded and unguarded children) at rate ρ per bonded/unreceptive female, which includes time spent pregnant or lactating. We can think of $\frac{1}{\rho}$ as the inter-birth interval, and $\sigma - \rho$ can be thought of as the probability that an unreceptive female will become receptive again without producing a child. Note that in our model females in the F^G and F^M pools are *producing* offspring (as opposed to necessarily having current dependents), and even if they retire or die, we assume that any children born are cared for until maturity or death. That is, our model assumes that all care required by a child is provided, no matter how much or how little that is.

Once a searching male has recruited a receptive female, he stops searching and invests his energy in guarding, so as to be assured of the paternity of the children his mate produces, and stops seeking other mates. Multiple-mating males, however, return immediately to the same pool to search for other mates. The kinetics of this mating model are as follows:

$$\begin{aligned} F + G &\underset{\beta}{\overset{r}{\rightleftharpoons}} F^G \xrightarrow{\rho} F^G + C^G, \\ F + M &\underset{\sigma-\rho}{\overset{r}{\rightleftharpoons}} F^M + M \xrightarrow{\rho} F + M + C^M. \end{aligned}$$

However; multiple maters may attempt to steal paternities from males in guarded pairs, and succeed at rate g per multiple mater. This is illustrated in the following diagramme:

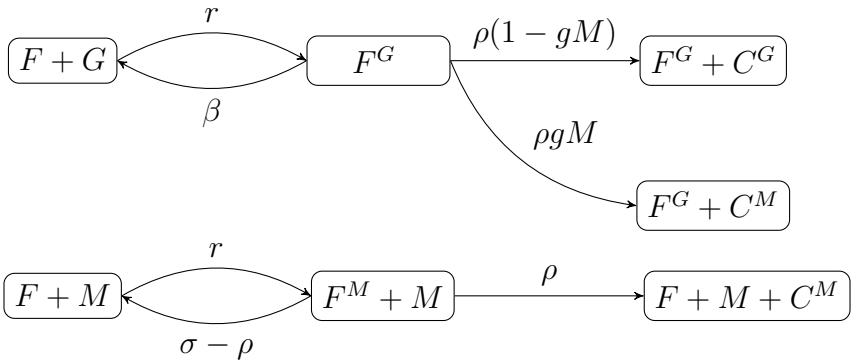

Together, β and g constitute an "effectiveness of guarding": β relates to the ability of guarding males to retain their mates for extended periods of time, and g relates to their ability to ensure that the children born to their female partners are indeed their own.

Finally, we include a population-density-dependent death rate νP, so that population growth is constrained. Removal due to the population density dependence does not have to be considered as death, but could also represent migration away from the population of interest. At this point, we can write the equations. A dot denotes a time derivative.

$$\begin{aligned} \dot{F} &= \frac{1}{2}\gamma\left(C^G + C^M\right) + \left(\beta + \lambda + \mu\left(k + \nu P\right)\right)F^G + \sigma F^M - \left(r\left(G + M\right) + \tau + \mu\left(1 + \nu P\right)\right)F, \\ \dot{G} &= \frac{1}{2}\gamma C^G + \left(\beta + \tau + \mu\left(1 + \nu P\right)\right)F^G - \left(rF + \lambda + \mu\left(k + \nu P\right)\right)G, \\ \dot{M} &= \frac{1}{2}\gamma C^M - \left(\lambda + \mu\left(k + \nu P\right)\right)M, \\ \dot{F}^G &= rFG - \left(\beta + \tau + \lambda + \mu\left(1 + k + 2\nu P\right)\right)F^G, \\ \dot{F}^M &= rFM - \left(\sigma + \tau + \mu\left(1 + \nu P\right)\right)F^M, \\ \dot{C}^G &= \rho\left(1 - gM\right)F^G - \left(\gamma + \delta\left(1 + \nu P\right)\right)C^G, \\ \dot{C}^M &= \rho\left(F^M + gMF^G\right) - \left(\gamma + \delta\left(1 + \nu P\right)\right)C^M. \end{aligned} \tag{1}$$

In words, this is

$$\dot{F} = \begin{bmatrix}\text{rate female}\\ \text{children mature}\end{bmatrix} + \begin{bmatrix}\text{rate guarded pairs}\\ \text{break spontaneously or}\\ \text{by death or retirement}\end{bmatrix} + \begin{bmatrix}\text{rate unreceptive}\\ \text{females return}\end{bmatrix} - \left(\begin{bmatrix}\text{rate receptive}\\ \text{females recruited}\\ \text{by males}\end{bmatrix} + \begin{bmatrix}\text{rate receptive}\\ \text{females retire}\\ \text{or die}\end{bmatrix}\right),$$

$$\dot{G} = \begin{bmatrix}\text{rate guarded}\\ \text{children mature}\end{bmatrix} + \begin{bmatrix}\text{rate guarded pairs}\\ \text{break spontaneously or}\\ \text{by death or retirement}\end{bmatrix} - \left(\begin{bmatrix}\text{rate guarded}\\ \text{pairs form}\end{bmatrix} + \begin{bmatrix}\text{rate guarding}\\ \text{males retire}\\ \text{or die}\end{bmatrix}\right),$$

$$\dot{M} = \begin{bmatrix}\text{rate unguarded}\\ \text{children mature}\end{bmatrix} - \begin{bmatrix}\text{rate multiple-}\\ \text{maters retire}\\ \text{or die}\end{bmatrix},$$

$$\dot{F}^G = \begin{bmatrix}\text{rate guarded}\\ \text{pairs form}\end{bmatrix} - \begin{bmatrix}\text{rate guarded}\\ \text{pairs break}\end{bmatrix},$$

$$\dot{F}^M = \begin{bmatrix}\text{rate receptive}\\ \text{females recruited}\\ \text{by multiple maters}\end{bmatrix} - \begin{bmatrix}\text{rate unreceptive}\\ \text{females return,}\\ \text{retire or die}\end{bmatrix},$$

$$\dot{C}^G = \begin{bmatrix}\text{rate guarded}\\ \text{children are born}\end{bmatrix} - \begin{bmatrix}\text{rate guarded}\\ \text{children mature or die}\end{bmatrix},$$

$$\dot{C}^M = \begin{bmatrix}\text{rate unguarded}\\ \text{children are born,}\\ \text{including paternity theft}\end{bmatrix} - \begin{bmatrix}\text{rate unguarded}\\ \text{children mature or die}\end{bmatrix}.$$

Children of multiple maters born to guarded females are automatically classified as unguarded (due to the terms $\pm gMF^G$ in the last two lines of Equation (1) above, indicating paternity theft), because the model tracks paternity rates explicitly. This means a reduction in the rate at which guarded children are born and a corresponding increase in the rate at which unguarded children are born when both g and M are not zero.

3. Life history

Our principal interest is in understanding the relative success of alternative strategies depending on fertility and mortality parameters, and guarding effectiveness. Mortality rates at all ages determine the average longevities, but we are interested in what strategy (or balance of strategies) might be chosen by populations with given longevities. Dividing the population into fertile/eligible adults and children imposes a minimal age structure, which we can conveniently use to reframe the parameters. We wish to exchange μ, δ and γ for parameters that characterise certain aspects of life history and environment.

Our model takes advantage of the elegance and simplicity of ODEs to achieve its goals. As such, it is not the same as an age-structured PDE model, although it contains a basic age structure which we shall use. We have two compartments representing children and five compartments representing adults. Individuals begin in a child compartment and move to an adult compartment at some time in the interval $(0, \infty)$ to take part in the adult dynamics that are of interest. As a result, some individuals can transition into adulthood at arbitrarily low age, and some individuals can remain children for an arbitrarily long time; in a certain sense, an

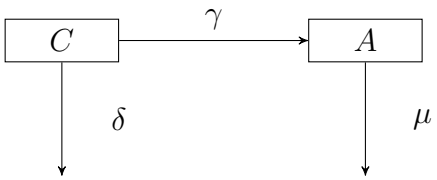

Figure 2: Block diagram of the age structure model governed by Equations (2).

ODE system such as this can only speak in terms of probabilities and of average times. Later work may introduce explicit age structure in an attempt to build in more realism.

If we consider only females and combine all female children and all female adults into respective groups C and A, and consider only the dynamics of maturation (due to γ) and the linear death rates δ and μ independent of population density (otherwise due to ν), we can extract dynamics that represent, in some sense, the female survivorship and the demographic distribution (between children and adults) of the female population of age t. This maturation and death dynamic is illustrated in Figure 2, where the transition from C to A is governed by a probabilistic rate γ, rather than a strict time (as in a model with more detailed ageing dynamics). These dynamics will be governed by differential equations

$$\begin{aligned} \frac{dC}{dt} &= -(\delta+\gamma)C, \\ \frac{dA}{dt} &= \gamma C - \mu A, \end{aligned} \tag{2}$$

and we will take initial conditions $C(0) = 1$ and $A(0) = 0$. The maturation rate γ causes a smooth increase in the number of adults up to the age

$$t^* = \frac{\ln \frac{\delta+\gamma}{\mu}}{\gamma+\delta-\mu}$$

satisfying $\frac{dA}{dt} = 0$, after which the decrease is monotonic towards 0 as t increases without bound. The child group is always monotonically decreasing at rate $\delta+\gamma$ as some individuals die (at rate δ) and some transition to adulthood (at rate γ).

Because we take the initial conditions of Equations (2) such that $C(0) + A(0) = 1$, the sum $S(t) := C(t) + A(t)$ represents the probability of an individual surviving to age t, depicted in Figure 3 as the solid curve. Note that $S(t)$ is a strictly decreasing function for $t \geq 0$, whose limit is 0 as $t \to \infty$. The ratio $\frac{A(t)}{S(t)}$ is the probability that a surviving individual has transitioned into adulthood by age t; it is a simple exercise to check that this expression has a limiting value of 1 as $t \to \infty$ when $\delta+\gamma > \mu$,[1] and by construction the mean transition time to adulthood is $\frac{1}{\gamma}$. Also depicted in the figure is $A(t)$ (dotted curve) and a representation of $C(t)$ as the vertical distance between the solid and dotted curves.

The expected time an individual lives in the population is

$$L = \int_0^\infty S(t)\, dt = \frac{\gamma+\mu}{\mu\,(\delta+\gamma)}.$$

We impose the constraint $t^* = \frac{L}{2}$, so that the peak of the curve $A(t)$ will always occur before $t = L$ (thus most of those surviving at age L have transitioned into adulthood). We impose

[1]The case where $\delta+\gamma < \mu$ is not of interest to our particular study, as adult mortality is generally lower than childhood mortality, but in that case the limiting ratio of adults over adults and children is $\frac{\gamma}{\mu-\delta}$.

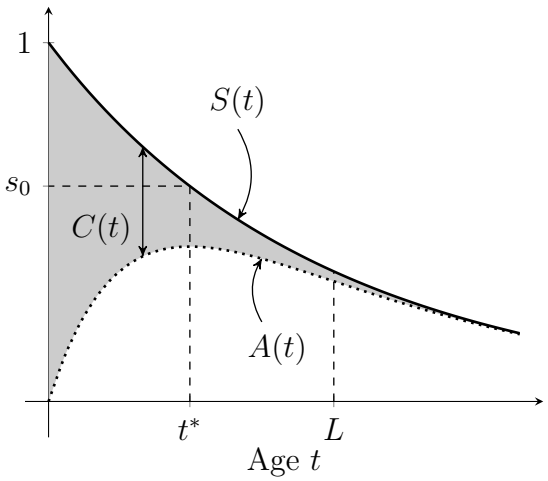

Figure 3: A typical example of $S(t)$ (solid curve). The dotted curve shows $A(t)$, indicating the demographic breakdown of individuals of age t, split between children and adults. The grey shaded region indicates children: initially all individuals are children, who decrease exponentially as age $t \to \infty$ according to $\exp(-(\delta+\gamma)t)$ (either through transition into adulthood or death). The number of adults peaks at t^*, and the total proportion surviving at that age is $s_0 = S(t^*)$.

another constraint that by age t^* a proportion $s_0 \in (0,1)$ are surviving, or that $s_0 := S(t^*)$. The purpose of these constraints is to introduce parameters characterising certain aspects of the population: t^* is a natural age (in the context of the model) to consider the "typical age of maturity"; s_0 characterises something of the "toughness" of being a juvenile; and L characterises the average life span of an individual.

Our constraints and the definition of L give us a system of equations

$$\begin{aligned} t^* &= \frac{\ln \frac{\delta+\gamma}{\mu}}{\gamma+\delta-\mu}, \\ s_0 &= S(t^*), \\ L &= \frac{\gamma+\mu}{\mu\,(\delta+\gamma)}, \end{aligned} \tag{3}$$

from which we can numerically obtain values of γ, δ and μ, given an expected life span L and survival rate s_0 at age t^*. The inversion fails if $s_0 > \frac{2}{e} \approx 0.736$ (where e is the base of the natural logarithm), though this is not problematic as the populations we attempt to model typically have survival rates of around 50% at maturity. Because we have constrained t^* to depend linearly on L, we now have that the three parameters δ, γ and μ are determined by only L and s_0.

As adult males are subject to base mortality rate $k\mu$, they suffer life expectancy at birth $\tilde{L} = \frac{\gamma+k\mu}{k\mu(\delta+\gamma)}$. Their relative life expectancy at birth is $\frac{L}{\tilde{L}} = \frac{\gamma+k\mu}{k(\gamma+\mu)}$.

Adult females have a fertile window of $t_1 - t^*(L)$; we can thus set $\tau(L,t_1) = \frac{2}{2t_1-L}$. Similarly, males have an eligible window of $t_2 - t^*(L)$; and so we set $\lambda(L,t_2) = \frac{2}{2t_2-L}$. For our purposes, we choose $t_1 = 45$ for the age of female fertility ends, and $t_2 = 75$ for the age of male retirement. While male chimpanzees cannot expect to live until such ages, such a high retirement age ensures that most low-longevity males will be removed by death, rather than retirement. In reality, it is likely that the age of male retirement is coupled somehow to longevity (as would be the age of female retirement/menopause in all primates but humans), but for the purposes of exploration in this model we keep these parameters decoupled.

Table 2: List and descriptions of all parameters. Some parameters are chosen zero during initial analysis.

Parameter	Typical value/range	Description
L	10 to 50	Mean female longevity
s_0	$\frac{1}{3}$ to $\frac{2}{3}$	Proportion of children surviving to adulthood
t_1	30 to 60	Age female fertility ends
t_2	60 to 80	Age of male retirement
ρ	$\frac{1}{4}$ to $\frac{1}{2}$	Rate children are born to guarded and unreceptive females
ν	$\frac{1}{1500}$ to $\frac{1}{500}$	Population-density-dependent death rate
r	$\frac{1}{2}$ to 2	Couple-forming rate
g	0 to 0.015	Paternity theft success rate per multiple-mating male
β	0 to $\frac{1}{4}$	Break-up rate for guarded pairs
σ	$\frac{1}{2}$ to 2	Re-availability rate for F^M females
k	0.9 to 1.1	Male death rate modifier
τ	see Table 3	Rate of menopausal retirement
λ	see Table 3	Male retirement rate

Table 3: Life history functions.

Parameter	Functional form	Description
$t^*(L)$	$\frac{L}{2}$	Age number of adults is maximal
$\gamma(L, s_0)$	Determined numerically from (3)	Maturation rate of children into adults
$\delta(L, s_0)$	Determined numerically from (3)	Base child death rate
$\mu(L, s_0)$	Determined numerically from (3)	Base death rate of adults
$\tau(L, t_1)$	$\frac{1}{t_1 - t^*(L)}$	Transition rate of fertile females to post-fertile
$\lambda(L, t_2)$	$\frac{1}{t_2 - t^*(L)}$	Transition rate of eligible males to ineligible

The original parameters involved in life history (γ, δ, μ, τ, λ) may now be replaced by expressions involving (L, s_0, t_1, t_2). Although k affects the life span of males, we place it among the parameters we consider to represent behavioural aspects of the biology, (r, g, β, σ, k). The remaining two parameters, (ρ, ν) we consider ecological/biological not related directly to life history or behaviour (as far as this study goes). Table 2 lists and describes all parameters and typical values or ranges that we explore, and Table 3 lists the mortality and other life history functions.

Parameters can be grouped according to three broad themes: life history, (L, s_0, t_1, t_2); behaviour, (r, g, β, σ, k); and environment/biology, (ρ, ν).

3.1. Adult sex ratio (ASR)

The adult sex ratio (ASR) is defined as the ratio of fertile males to fertile females. Our model assumes all adult males are fertile. Thus the ASR a is given by

$$a = \frac{\bar{M}}{\bar{F}}.$$

The hypothesis of [2] regarding humans, also the subject of [7, 8, 9] is that the ASR determines male mating strategy. We aim to investigate whether the ASR is a sufficient index to determine the strategy (when there are two strategies in play) or if other parameters are necessary.

The model dynamics cause us to predict that increasing t_1 will decrease the ASR by causing females to remain fertile for longer, and thus increase relative to the number of eligible males. Similarly, increasing t_2 will increase the ASR by increasing the relative number of eligible males to fertile females. Increasing time that individuals are in the population L (independently of t_1 and t_2) should increase the effect of disparity between t_1 and t_2, so with $t_2 > t_1$, higher L should increase the ASR. This is a consequence of the model; for if $t_2 \gg t_1 \gg t^*$, then $\frac{1}{t_2 - t^*} \ll \frac{1}{t_1 - t^*}$, and this may in turn be much smaller than μ or $k\mu$. This higher value of μ or $k\mu$ removing individuals by death would effectively swamp the effect of removal due to retirement. For given time L that individuals are in the population, increasing $s_0 \in [\frac{1}{3}, \frac{2}{3}]$ increases μ and thus should tend the ASR towards 1. Naturally, increasing k should decrease the ASR by selectively removing males earlier.

4. Numerical investigations

We explore our model in two ways, both using Matlab's `ode15s` function to integrate system (1) numerically, ensuring that all variables remain non-negative. The first exploration is to straightforwardly study the parameter landscape on grids varying two life history parameters (L and t_1), with other parameters fixed at various choices. The second is a broader sensitivity analysis varying all parameters within reasonable ranges, allowing us to assess how each parameter influences ASR and dominant strategy.

4.1. Method and results

We generate a grid on the parameter space and examine the resulting ASR and strategy contours in the plane whose axes are L and t_1 (the Lt_1-plane), illustrated in Figures 4-7. We show several slices of the grid for different paternity theft and pair-bond break-up rates (assessing the behaviour with regard to effectiveness of guarding). The four figures show the results for all combinations of $t_2 \in \{60, 80\}$ and $k \in \{1, 1.2\}$. Each figure shows a grid of six contour plots (landscapes) for paternity theft rate $g = 0$ or 0.003, and pair-bond break-up rates $\beta = 0$, $\frac{1}{16}$, and $\frac{1}{4}$. Each landscape has an "extinction boundary" along the bottom and left of the image, where either menopause or death occurs at such a low average age that the average number of offspring per female is below replacement levels with the given mean birth rate $\rho = \frac{1}{3}$. In general, there is a clear boundary between regions of the Lt_1 plane where one strategy dominates over the other; except near the extinction boundary to the lower left in some of the landscapes, this boundary has a positive gradient. Contours of constant ASR are generally of positive gradient also. This observation is to be expected, as with increasing age female fertility ends t_1, the number of fertile females relative to eligible males increases; and as life expectancy at birth increases, the adult death rate μ decreases, causing females and male retirement rates τ and λ to dominate in the removal of fertile/eligible adults from the population, increasing the ASR when $t_1 < t_2$. Rephrasing the preceding logic, high adult mortality swamps removal by retirement; conversely, low adult mortality makes visible any differences between t_1 and t_2. In these plots, we do not have $t_1 > t_2$, so only positive-gradient contours are visible; had we explored either lower t_2 or higher t_1, negative-gradient contours would appear.

There is a tipping point where either life expectancy at birth L increases sufficiently or age female fertility ends t_1 decreases sufficiently that guarding takes over from multiple mating.

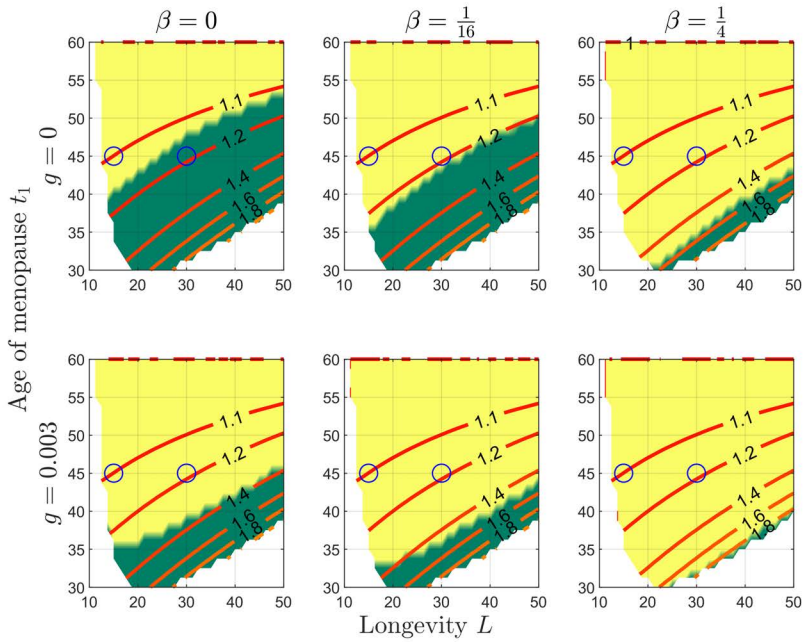

Figure 4: Contour plots of solution outcomes in the Lt_1-plane for $g = 0$ (top row) and $g = 0.003$ (bottom row), and $\beta = 0$ (left column), $\beta = \frac{1}{16}$ (middle column), $\beta = \frac{1}{4}$ (right column). White background indicates extinctions, dark/green indicates guarding dominates, light/yellow indicates multiple mating dominates. Labelled contours indicate contours of constant ASR. Other parameter values are fixed: $s_0 = \frac{1}{2}$, $t_2 = 60$, $\rho = \frac{1}{3}$, $\nu = 0.001$, $r = 2$, $\sigma = 1$, $k = 1$. Blue circles indicate approximate locations of chimpanzee and hunter-gatherer life histories at $(L, t_1) \approx (15, 45)$, $(30, 45)$ respectively.

Increasing either the pair-bond break-up rate β or the paternity theft rate g increases the proportion of the landscape that is taken up by multiple mating.

Figure 4 shows landscapes for age of male retirement $t_2 = 60$, male-specific mortality risk $k = 1$. Observe that because the male-specific mortality risk $k = 1$ and age of male infirmity $t_2 = 60$, along the line with age female fertility ends $t_1 = 60$ we have ASR exactly equal to 1, as we should expect. We see in this set of landscapes that the contour along which strategy switches tends to stay very close to contours of constant ASR.

In Figure 5, the age of male infirmity remains 60, but male-specific mortality risk $k = 1.2$. This is accompanied by an increase in the approximate ASR at which strategy appears to switch. While again the switch in strategy does not lie strictly *on* a contour of constant ASR, it remains very near—arguably nearer than in Figure 4.

Figure 6 shows the same set of landscapes for $t_2 = 80$ and $k = 1$. The general features we observed earlier are largely the same, with the following exception: for $g = 0.003$, the contour along which strategy switches deviates markedly from the contours of constant ASR for low L and low t_1, near the extinction boundary. If observed closely, this detail may be seen in the corresponding row of Figure 4. This, we posit, is an artefact of our life history model: for sufficiently low L, adult life expectancy may decrease more slowly with L, leading to comparatively longer adult life expectancies, with the upshot that males can therefore expect a relatively longer time to compete for the comparatively quickly retiring females, and to gain paternities when pair-bonded.

Finally, Figure 7 has $t_2 = 80$ and $k = 1.2$. Because the male-specific mortality risk factor is higher than in Figure 6, multiple mating gains more traction in this instance; however, because the age of male infirmity is higher than it is in Figure 5, guarding has more traction than in that instance. Again, note that the strategy-switch contour lies very close to contours of constant

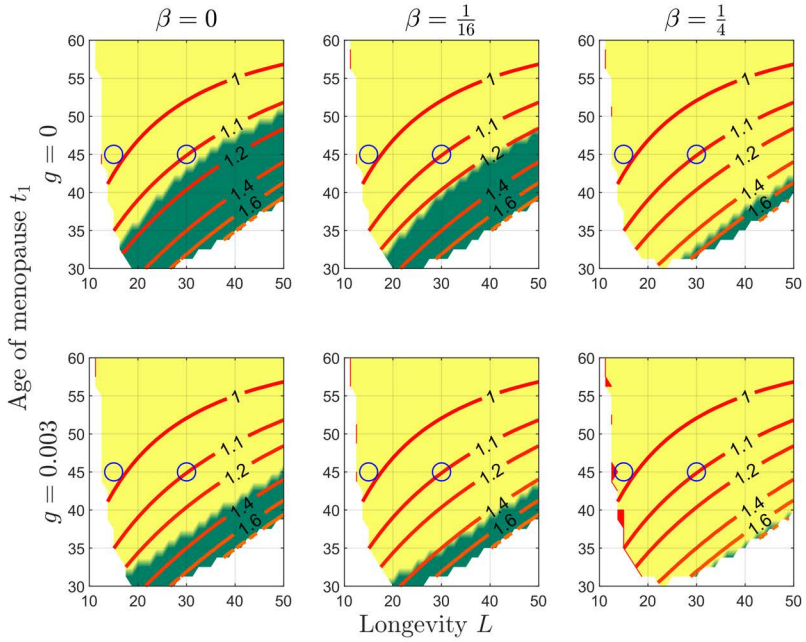

Figure 5: Contour plots of solution outcomes in the Lt_1-plane for $g = 0$ (top row) and $g = 0.003$ (bottom row), and $\beta = 0$ (left column), $\beta = \frac{1}{16}$ (middle column), $\beta = \frac{1}{4}$ (right column). White background indicates extinctions, dark/green indicates guarding dominates, light/yellow indicates multiple mating dominates. Labelled contours indicate contours of constant ASR. Other parameter values are fixed: $s_0 = \frac{1}{2}$, $t_2 = 60$, $\rho = \frac{1}{3}$, $\nu = 0.001$, $r = 2$, $\sigma = 1$, $k = 1.2$. Blue circles indicate approximate locations of chimpanzee and hunter-gatherer life histories at $(L, t_1) \approx (15, 45)$, $(30, 45)$ respectively.

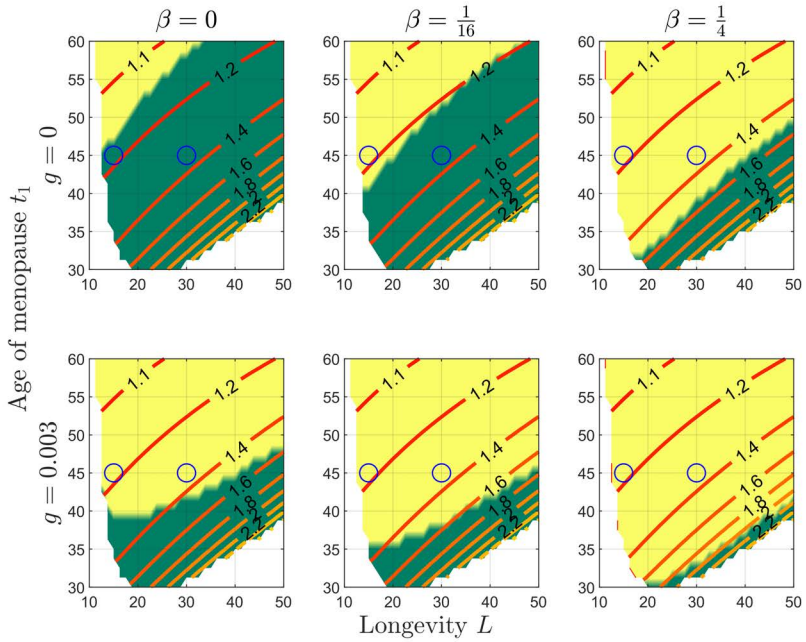

Figure 6: Contour plots of solution outcomes in the Lt_1-plane for $g = 0$ (top row) and $g = 0.003$ (bottom row), and $\beta = 0$ (left column), $\beta = \frac{1}{16}$ (middle column), $\beta = \frac{1}{4}$ (right column). White background indicates extinctions, dark/green indicates guarding dominates, light/yellow indicates multiple mating dominates. Labelled contours indicate contours of constant ASR. Other parameter values are fixed: $s_0 = \frac{1}{2}$, $t_2 = 80$, $\rho = \frac{1}{3}$, $\nu = 0.001$, $r = 2$, $\sigma = 1$, $k = 1$. Blue circles indicate approximate locations of chimpanzee and hunter-gatherer life histories at $(L, t_1) \approx (15, 45)$, $(30, 45)$ respectively.

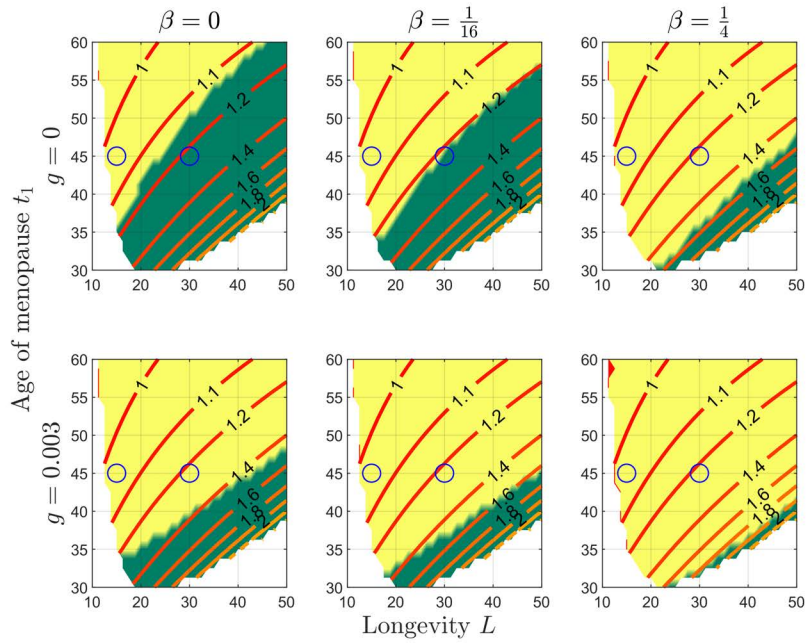

Figure 7: Contour plots of solution outcomes in the Lt_1-plane for $g = 0$ (top row) and $g = 0.003$ (bottom row), and $\beta = 0$ (left column), $\beta = \frac{1}{16}$ (middle column), $\beta = \frac{1}{4}$ (right column). White background indicates extinctions, dark/green indicates guarding dominates, light/yellow indicates multiple mating dominates. Labelled contours indicate contours of constant ASR. Other parameter values are fixed: $s_0 = \frac{1}{2}$, $t_2 = 80$, $\rho = \frac{1}{3}$, $\nu = 0.001$, $r = 2$, $\sigma = 1$, $k = 1.2$. Blue circles indicate approximate locations of chimpanzee and hunter-gatherer life histories at $(L, t_1) \approx (15, 45)$, $(30, 45)$ respectively.

ASR.

The broad results indicate that in a landscape with varying life expectancy L and age female fertility ends t_1 four things are of note:

1) multiple mating dominates when the average length of time that males can compete decreases (either by increasing the male-specific mortality risk k or decreasing the age of male retirement t_2);

2) ASR increases when male retirement is later in life, and when male-specific mortality is lower;

3) improving the effectiveness of guarding increases the region of the Lt_1-plane where guarding dominates; and

4) the boundary between multiple mating and guarding aligns well, overall, with contours of constant ASR in the Lt_1-plane, indicating that the "signal" of dominant male strategy as a function of ASR does not depend very much on life history parameters, but does depend on behavioural parameters such as paternity theft rate and the average length of time a pair bond lasts.

Point 1 above indicates that given a fixed effectiveness of guarding, the length of time that males are able to compete for paternities determines how they are best able to maximise their average number of paternities. Less time means spreading risk across multiple mates, and more time means investing in a single mate.

Assuming that all other parameters are constant, it may be possible to shift from multiple mating to guarding as the dominant male strategy just by increasing life expectancy at birth, a manoeuvre that simultaneously increases the ASR when $t_1 < t_2$. A plausible instance of this

idea would be to draw a path connecting the two circles in the upper-middle plot of Figure 7, which has pair-bond break-up rate $\beta = \frac{1}{16}$ and paternity theft rate $g = 0$. One might imagine that our common ancestor with chimpanzees (as close as can be represented in a model such as this) lived near the point with $L = 15$ and $t_1 = 45$, and a "short" evolutionary trajectory that increased only our life span (as far as this model's parameters are concerned, i.e. with no increase in age that female fertility ends) could have tipped us from multiple mating into guarding male mating strategies.

4.2. Sensitivity analysis

We use Latin hypercube sampling to generate 100 000 parameter points within reasonable ranges. We take age female fertility ends t_1 between 40 and 55, age of male retirement t_2 between 60 and 80, birth frequency ρ between $\frac{1}{3.5}$ and $\frac{1}{2.5}$, and male relative risk k between 1 and 1.2, and excluding cases where the resulting ASR was outside the range of $\frac{1}{3}$ to 3. All other parameter ranges are as specified in Table 2. Results are given shown in Table 4, including p-values, for the 54 082 points that satisfy the ASR requirement.

Of particular note are the following observations:

1. As expected, life history parameters (L, s_0, t_1, t_2)—respectively life expectancy at birth, proportion of children surviving to adulthood,[2] age female fertility ends, and age of male infirmity—correlate very strongly with ASR; male specific mortality risk k and birth rate ρ have moderate correlations with ASR; all other parameters correlate very little.
2. Only s_0 and t_1, of the life history parameters, correlate moderately with with dominant strategy; L and t_2 have only very small correlations with strategy.
3. Paternity theft g is the most important factor in determining the dominant strategy.
4. Mean birth rate ρ and population density dependent death rate ν have weak to moderate correlations with strategy, while mean pair-bond break-up rate β and return time σ are only weakly correlated with changes in dominant strategy. Interestingly, the male-specific mortality risk factor k has almost no effect on dominant strategy.

Results relevant to Table 4 are shown graphically in Figures 8-9. Figure 8 shows how the ASR and dominant strategy (or strategy balance) cluster according to varying parameters of the model. The horizontal axes indicate the dependent quantities (fraction multiple mating and ASR), while the vertical axis indicates one of the parameters, of which we illustrate in the subfigures L, t_1, t_2, g, β, and k. Each point corresponds to the outcome for a given set of parameters. No set of parameters that we found resulted in a coexistence equilibrium, so the fraction multiple mating is always either 0 (all guarding at equilibrium) or 1 (all multiple mating at equilibrium). Yellow diamonds correspond to parameter sets with $L < 25$, and blue discs correspond to parameter sets with $L \geq 25$.

In particular, Subfigures 8a and 8b show how (a) ASR tends to increase as L increases, and (b) ASR tends to decrease as t_1 increases. The figures show clouds of points that either spread out or contract along the ASR axis as either L or t_1 increases (respectively). In Subfigure 8b it is also possible to observe that the density of points along the face with all males guarding

[2]To clarify why this should be expected to have an effect, holding L constant and increasing s_0, we simultaneously increase δ and decrease μ. As a result, with both $t_1 < t_2$ constant, changes in μ resulting from changes in s_0 result in a change in ASR due to the difference in values of t_1 and t_2.

Table 4: Spearman partial rank correlation coefficients for ASR and fraction of multiple maters, and corresponding p-values.

Variable	ρ_{ASR}	p_{ASR}	ρ_{Mratio}	p_{Mratio}
L	0.877 82	0	0.070 436	1.9494×10^{-60}
s_0	−0.772 77	0	0.410 73	0
t_1	−0.957 76	0	0.398 01	0
t_2	0.655 21	0	−0.035 419	1.7428×10^{-16}
ρ	−0.476 89	0	0.360 25	0
ν	0.032 229	6.5729×10^{-14}	−0.302 99	0
r	−0.010 885	0.011 367	−0.006 190 7	0.15
g	−0.077 788	2.4103×10^{-73}	0.8229	0
β	−0.011 31	0.008 538 4	0.100 41	3.536×10^{-121}
σ	0.019 337	6.9011×10^{-6}	−0.126 14	1.2897×10^{-190}
k	−0.566 76	0	0.023 348	5.6397×10^{-8}

decreases as t_1 increases, corresponding to a relative increase in the rate of multiple mating as t_1 increases.

Subfigures 8c to 8f depict the same type of information, but for different parameters, respectively illustrating the changes in ASR and dominant strategy with respect to t_2, g, β and k. In Subfigure 8c we can see the more constrained (and opposite direction) change in typical ASR as t_2 increases, compared to that with t_1, while the relatively consistent densities of points at t_2 increases reflect the very little relationship between changes in t_2 and the strategy balance. The male mortality risk factor k similarly results in a moderately monotonic change in ASR with little associated change in dominant strategy.

We see a slightly different pattern in Subfigures 8d and 8e, in which changes in the parameter result in very little monotonic change in ASR, but a notable change in the dominant strategy. Changes in paternity theft rate g directly affect the successfulness of guarding, and so as a result the density of the "guarding cloud" decreases as g increases in Subfigure 8d, and the width of the "multiple mating cloud" in the ASR direction increases (thus little overall monotonic trend for change in ASR with change in g). The picture in Subfigure 8e is similar, in that the density of the "guarding cloud" decreases with increasing pair-bond break-up rate β, as guarded females tend to move into the receptive pool on average sooner, making them available for multiple maters to recruit.

In Figure 9, red diamonds indicate parameter points for which guarding dominates, while blue dots indicate parameter points for which multiple mating dominates, and the axes are Longevity L, age that female fertility ends t_1 and ASR. Observe that while ASR can be very high for some points with high L and low t_1, and multiple mating can dominate for some points in this regime (unrealistic for any mammal, in fact), the points for which guarding dominates largely form a "blanket" over those for which multiple mating wins, and do not appear to occur with great frequency in the low L-high t_1 regime. ASRs are generally around 1 in the low L-high t_1 regime because males do not on average get to live long enough for any difference between male and female retirement ages to make much difference to the ASR. Observe that there is a low density of ASRs for which guarding wins below approximately 1.2. In contrast, multiple mating occurs quite densely in parameter regions associated with lower ASRs. The boundary below which no guarding occurs is close to (but not exactly) a horizontal plane.

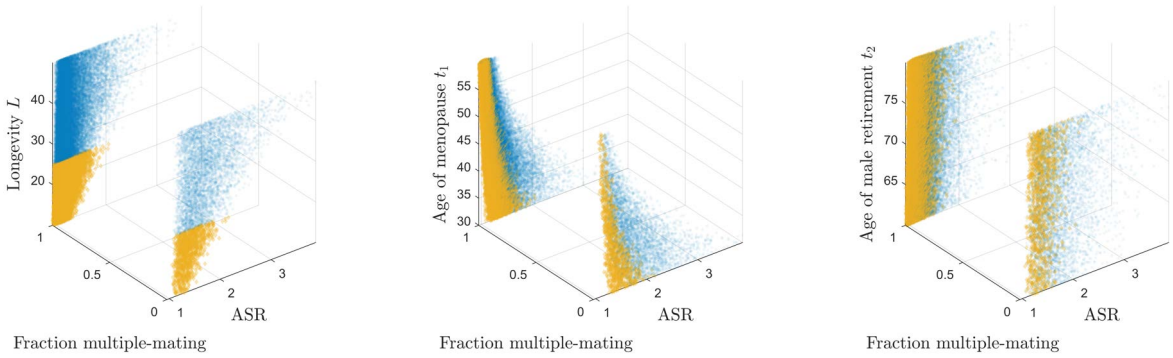

(a) L **(b)** t_1 **(c)** t_2

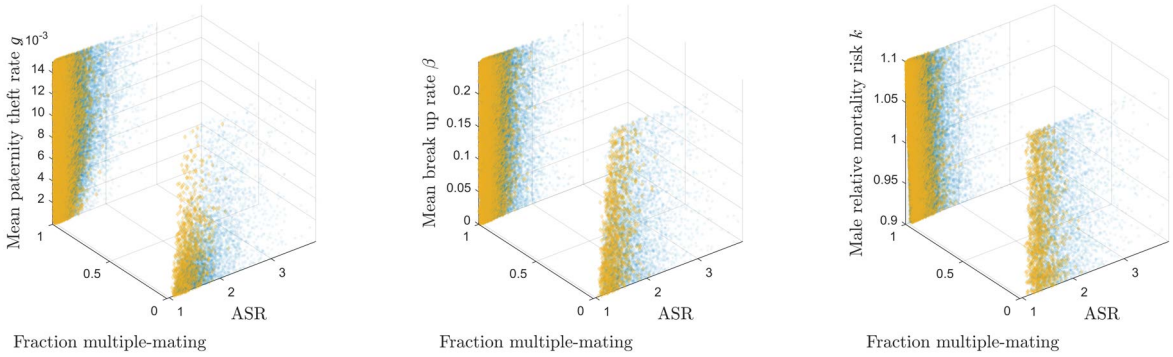

(d) g **(e)** β **(f)** k

Figure 8: Scatter plots of a subset of parameters versus ASR and fraction of males multiple-mating. Blue dots: parameter points where life expectancy at birth $L > 25$. Yellow diamonds: parameter points where life expectancy at birth $L < 25$.

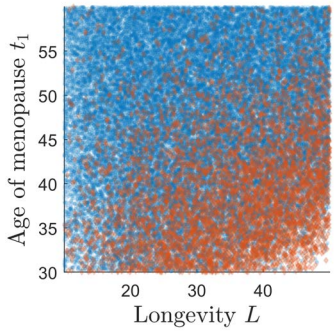

(a) xy

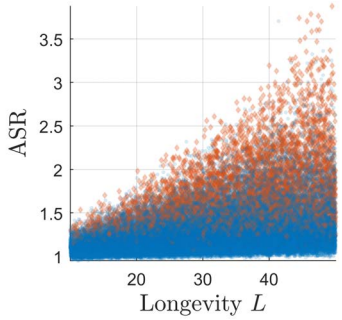

(b) xz

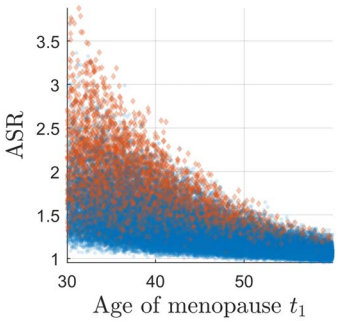

(c) yz

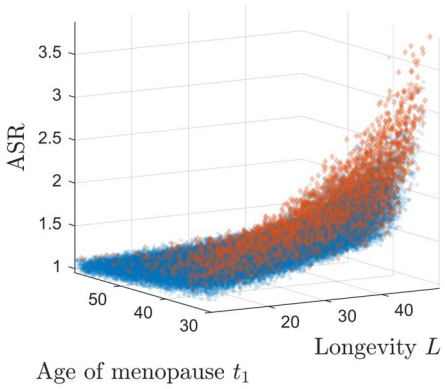

(d) xyz

Figure 9: Scatter plots of ASR versus life expectancy at birth L and age female fertility ends t_1. Blue dots: parameter points where multiple mating dominates. Red diamonds: parameter points where guarding dominates. Observe that guarding is rare below ASR ≈ 1.5.

4.3. Discussion

The result noted in point 1 of Subsection 4.2 that birth rate ρ affects ASR anything more than weakly (or at all) may be considered surprising, as more children born would not result in a difference in sex ratios at the point where they transition to adulthood, and the proportion of adult males and females in the population should not shift as a result of changing the birth rate alone. We surmise that the effect is due to the population-density-dependent death rates: females are removed according to $\mu(1 + \nu P)$ per head, but males are removed according to $\mu(k + \nu P)$ per head. That is, given a total population P, the population-density-dependent removal per individual is the same; given equal numbers of males and females, removal due to population density is at the same rate, but removal specifically due to death independent of population density is higher for males. With a higher birth rate, we expect the population to reach its carrying capacity more quickly, and thus for males to tend to be removed more quickly due to the factor $k \geq 1$, reducing the ASR. Moving k so that males are subject to removal according to $k\mu(1 + \nu P)$ per head or considering $k < 1$ would make ASR less sensitive to changes in ρ.

The correlation of birth rate ρ to strategy is less surprising: a higher birth rate implies more opportunities for paternity *and* paternity theft [3], hence increasing ρ tends to increase the frequency of multiple mating as dominant strategy. However, controlling for the paternity theft rate g, the rank correlation between ρ and multiple mating as dominant strategy is still 0.2262—weaker than before, but still far from negligible, indicating that though paternity theft contributes to the increasing success of multiple mating with increasing ρ, it is not the only factor. The likely underlying cause is the fact that multiple maters can recruit multiple females at once; increasing the average number of offspring per recruitment is therefore a significant advantage if you do not restrict yourself to a single female as guarders do.

In Chimpanzees, the inter-birth interval is approximately four to five years, but in humans it is on average less than three—very surprising for a species of our longevity. The Grandmother Hypothesis posits that grandmothering subsidies for their daughters' child-rearing could shorten it, while retaining the ancestral age of that female fertility ends. The difference in inter-birth interval thus suggests in our model that humans should possibly be more likely to multiple-mate than chimps, but the weakness of the correlation and differences in other parameters tending towards the success of guarding may be sufficient to compensate. A further difference is that most male chimpanzees are dead by t_1, thus having a much shorter typical period in which to compete for paternities.

Similarly surprising is the dependence of dominant strategy on ν. As $\frac{1}{\nu}$ corresponds to the carrying capacity, increasing the carrying capacity (decreasing ν) appears to increase the success of multiple mating. We posit that this is because although the effect of changing ν on the ASR is minimal, the dominant strategy is strongly dependent on the number of receptive females at equilibrium. Consequently, it may be that as ν increases (corresponding to a decrease in the maximum population size), the number of receptive females decreases, meaning that fewer receptive females can be recruited by multiple maters, giving guarders an advantage as they obtain more assured paternities with what mates they can obtain and guard for an extended length of time.

Results indicated in Table 4 show that, in particular, the proportion s_0 of children surviving to age t^*, age t_1 that female fertility ends and per-female birth rate ρ have relatively strong positive correlations with ASR and negative with dominance of multiple mating, while other parameters correlate at most very weakly to either ASR or dominant strategy and weakly to strongly with the other, or neither. That is, changes in s_0, t_1 or ρ result in relatively strong changes in the balance between ASR and dominant strategy. Controlling for these three variables, the

Spearman partial rank correlation coefficient between ASR and dominance of multiple mating is -0.0345, indicating that there is at most only a very, very weakly monotonic relationship between ASR and dominant strategy under variation of all other parameters. That is, varying s_0, t_1 and ρ in particular causes ASR and strategy to covary in such a way as that ASR can be seen as an index for predicting—at least roughly—the dominant strategy. This result is consistent with the observations in Figures 4-7, where the contour along which dominant strategy switches is largely aligned with some contour of constant ASR.

What we can understand from Figures 9 and 8 is that there is no distinct value of ASR at which strategy switches in the full parameter space. ASR does, however, act as a guide: guarding does not appear to occur at all for parameter sets resulting in ASR below approximately 1.1, and for a given neighbourhood in Lt_1 space, parameters resulting in a higher ASR will tend to result in guarding dominating, while those resulting in a lower ASR will tend to result in multiple mating dominating. The boundary below which only multiple mating occurs decreases slightly in ASR as age female fertility ends increases; ASR in general *should* decrease as age female fertility ends increases (relative to age of male infirmity). As the ASR decreases, guarding becomes less frequent in the high age female fertility ends regime.

What we suggest guides the dynamic is that guarding becomes favourable when the female retirement time scale, $\frac{1}{\tau}$, is low enough that it becomes significant in causing retirements for females in the unreceptive F^M pool. A female recruited by a guarding male will typically produce $\frac{\rho}{\beta+\tau+\mu}$ offspring, compared to $\frac{\rho}{\sigma+\tau+\mu}$ for one recruited by a multiple mater. Increasing τ (the rate at which females advance to menopause) not only reduces the average length of time that females spend in either reproducing pool, but will reduce the number of receptive females for all males to recruit. However, guarding males who manage to recruit a receptive female are guaranteed a longer time with them to obtain paternities, but the success of multiple mating depends on both how many receptive females females and also on how many competitors there are: fewer possible recruitments drastically reduces the possible number of paternities, and thus guarding is more likely to out-compete multiple mating.

5. Conclusion

We have developed a parsimonious model for a primate-like population endowed with sufficient details about life history and behaviour to begin exploring mathematically the link between the ASR and the dominant strategy employed by males, and the elements of behaviour and biology that may affect the outcome to varying extents. We wish to use this model (or subsequent daughter models) to help explain behavioural differences between ourselves and our nearest living relatives, the chimpanzees, with the benefit that the model is general enough that the approach employed herein can be used to understand the mating strategy dynamics of other species as well. Our model does not assume anything about the details of male-male or male-female interactions—only their net outcomes as they relate to mean reproduction and mortality rates, though distinguishing $t_1 < t_2$ is a detail specific to humans.

Our results indicate that female scarcity relative to the length of the male's window of opportunity to reproduce strongly dictates the likelihood that guarding will take hold over multiple mating, given some understanding of how mate-guarding is accomplished. That is, given an estimate of the effectiveness of guarding (both in maintaining long term guarded relationships and in preventing paternity theft) and, in relevant species (such as humans) the lengths of the reproductive intervals of males and females, the ASR may provide an index by which to predict the typical mating strategy of males.

5.1. Extensions of the model

There are several further directions we wish to explore:

- Detailed inheritance models; females who latently carry strategy "genes" that determine their offspring's strategy in combination with their father's genes.
- Active strategy choice; males choose dynamically into which strategy to invest effort. Strategy choice may depend on the "mean" strategy adopted by the population.
- Additional strategies; for example, paternal carers, whose energy investment goes into ensuring that the offspring they care for have better survival rates.
- More detailed paternity theft; including opportunistic paternity-stealing by guarding males.

Acknowledgments

DR and PSK were supported by the Australian Research Council, Discovery Project (DP160101597).

Bibliography

[1] Blurton Jones, N. G. (2016). *Demography and evolutionary ecology of Hadza hunter-gatherers*, volume 71. Cambridge University Press, Cambridge.

[2] Coxworth, J. E., Kim, P. S., McQueen, J. S., and Hawkes, K. (2015). Grandmothering life histories and human pair bonding. *Proceedings of the National Academy of Sciences*, 112(38):11806–11811.

[3] Hawkes, K., Rogers, A. R., and Charnov, E. L. (1995). The male's dilemma: increased offspring production is more paternity to steal. *Evolutionary Ecology*, 9(6):662–677.

[4] Hill, K., Boesch, C., Goodall, J., Pusey, A., Williams, J., and Wrangham, R. (2001). Mortality rates among wild chimpanzees. *Journal of Human Evolution*, 40(5):437–450.

[5] Hill, K. and Hurtado, M. (1995). Ache life history: the ecology and demography of a foraging people.

[6] Howell, N. (1979). *Demography of the Dobe !Kung*. Academic Press, New York.

[7] Loo, S. L., Chan, M. H., Hawkes, K., and Kim, P. S. (2017a). Further mathematical modelling of mating sex ratios & male strategies with special relevance to human life history. *Bulletin of mathematical biology*, 79(8):1907–1922.

[8] Loo, S. L., Hawkes, K., and Kim, P. S. (2017b). Evolution of male strategies with sex-ratio–dependent pay-offs: connecting pair bonds with grandmothering. *Phil. Trans. R. Soc. B*, 372(1729):20170041.

[9] Schacht, R. and Bell, A. V. (2016). The evolution of monogamy in response to partner scarcity. *Scientific reports*, 6:32472.

[10] Schacht, R., Kramer, K. L., Székely, T., and Kappeler, P. M. (2017). Adult sex ratios and reproductive strategies: a critical re-examination of sex differences in human and animal societies. *Philosophical Transactions of the Royal Society B: Biological Sciences*, 372(1729).

[11] Tutin, C. E. G. (1979). Mating patterns and reproductive strategies in a community of wild chimpanzees (pan troglodytes schweinfurthii). *Behavioral Ecology and Sociobiology*, 6(1):29–38.